S-Allyl-L-Cysteine Sulfoxide Inhibits Tumor Necrosis Factor-Alpha Induced Monocyte Adhesion and Intercellular Cell Adhesion Molecule-1 Expression in Human Umbilical Vein Endothelial Cells

CHAI HUI,[1] WO LIKE,[2] FU YAN,[3*] XIE TIAN,[4] WANG QIUYAN,[4] AND HUANG LIFENG[4]

[1]College of Life Science, Zhejiang Chinese Medical University, Hangzhou, China
[2]The First Affiliated Hospital of Zhejiang Chinese Medical University, Hangzhou, China
[3]College of Animal Sciences, Zhejiang University, Hangzhou, China
[4]Center for Biomedicine and Health, Hangzhou Normal University, Hangzhou, China

ABSTRACT

Garlic and its water-soluble allyl sulfur-containing compound, *S*-Allyl-L-cysteine Sulfoxide (ACSO), have shown antioxidant and anti-inflammatory activities, inhibiting the development of atherosclerosis. However, little is known about the mechanism(s) underlying the therapeutic effect of ACSO in inhibiting the formation of atherosclerostic lesion. This study aimed to investigate whether ACSO could modulate tumor necrosis factor-alpha (TNF-α)-induced expression of intercellular cell adhesion molecule-1, monocyte adhesion and TNF-α-mediated signaling in human umbilical vein endothelial cells. While TNF-α promoted the intercellular cell adhesion molecule-1 mRNA transcription in a dose- and time-dependent manner, ACSO treatment significantly reduced the levels of TNF-α-induced intercellular cell adhesion molecule-1 mRNA transcripts ($P < 0.01$). Furthermore, ACSO dramatically inhibited TNF-α triggered adhesion of THP-1 monocytes to endothelial cells and porcine coronary artery rings. Moreover, ACSO mitigated TNF-α induced depolarization of mitochondrial membrane potential and overproduction of superoxide anion, associated with the inhibition of NOX4, a subunit of nicotinamide adenine dinucleotide phosphate-oxidase, mRNA transcription. In addition, ACSO also inhibited TNF-α-induced phosphorylation of JNK, ERK1/2 and IκB, but not p38. Apparently, ACSO inhibited proinflammatory cytokine-induced adhesion of monocytes to endothelial cells by inhibiting the mitogen-activated protein kinase signaling and related intercellular cell adhesion molecule-1 expression, maintaining mitochondrial membrane potential, and suppressing the overproduction of superoxide anion in endothelial cells. Therefore, our findings may provide new insights into ACSO on controlling TNF-α-mediated inflammation and vascular disease. Anat Rec, 293:421–430, 2010.

Key words: endothelial cells; *S*-Allyl-L-cysteine sulfoxide; tumor necrosis factor-alpha; intercellular cell adhesion molecule-1; superoxide anion; NADH oxidase

Chai Hui and Wo Like contributed equally to this work.

*Correspondence to: Fu Yan, College of Animal Sciences, Zhejiang University, Hangzhou 310029, China. Fax: 86-571-86044349. E-mail: fuyan@zju.edu.cn

Received 21 December 2008; Accepted 14 July 2009
DOI 10.1002/ar.21070
Published online 20 January 2010 in Wiley InterScience (www.interscience.wiley.com).

INTRODUCTION

Endothelial dysfunction in the arterial wall is associated with inflammation, which has been thought to trigger leukocyte adhesion, platelet aggregation, and vascular smooth muscle cell proliferation and migration, leading to thickening of the arterial wall and the formation of atherosclerotic lesion (Kaperonis et al., 2006). During the process of atherosclerosis, immune cells such as monocytes, macrophages, T and B cells can adhere onto endothelial cells and elicit acute coronary syndromes (Hansson, 2005). Furthermore, inflammatory cells can accelerate the formation of early atherosclerotic lesions through inflammatory molecules and cytokines. Tumor necrosis factor-alpha (TNF-α), a prototypic proinflammatory cytokine, has been demonstrated to induce the expression of cell adhesion molecules, such as intercellular cell adhesion molecule-1 (ICAM-1), on endothelial cells and facilitate the adhesion of leukocytes. And this adhesion process is crucial for the development of atherosclerosis (Migita et al., 2004; Suwannaprapha et al., 2005). Therefore, treatment with TNF-α antagonist or downregulation of ICAM-1 expression on endothelial cells may inhibit the adhesion of leukocytes and suppress the progression of atherosclerosis.

Garlic is a flavoring agent and has been used as a therapeutic supplement for treatment of many diseases for decades. Its therapeutic effect is attributed to its antioxidant and anti-inflammation activities (Salman et al., 1999, Helen et al., 2003). Garlic and its water-soluble allyl sulfur compound, *S*-Allyl-L-cysteine sulfoxide (ACSO), have been demonstrated to inhibit pathogenic parasites, worms, bacterial, and fungal infections (Migita et al., 2004). Furthermore, garlic and ACSO can also prevent the oxidation of human low density lipoprotein, decrease oxidative stress in smokers and reduce blood pressure, effectively lowing the levels of plasma cholesterol and triglycerides in hyperlipidemic human subjects and inhibiting the development of atherosclerosis (Hirsch et al., 2000; Allison et al., 2006). However, the mechanism(s) underlying the action of ACSO in inhibiting the development of atherosclerosis and preventing cardiovascular diseases is still poorly understood.

In this study, we hypothesized that ACSO pretreatment may affect TNF-α-induced endothelial damage through minimizing the oxidative stress and mitogen-activated protein kinase (MAPK) pathway activation. Specifically, the effects of ACSO treatment on ICAM-1 expression and monocyte adhesion were investigated. In addition, we also investigated the superoxide anion production, the expression of NADPH oxidase 4 (NOX-4) and mitochondrial potential as well as TNF-α-related signaling in human umbilical vein endothelial cells (HUVECs). This study may help us understand the mechanisms and also suggest potential therapeutic roles of ACSO in the treatment of cardiovascular disease.

MATERIALS AND METHODS

Endothelial Cell Culture

HUVECs were cultured with 10% heat-inactivated FBS EBM-2 medium at 37°C in a humidified atmosphere of 5% CO_2 in air. The cells at passage 4–6 were used for all experiments. Upon 80%–85% confluence, HUVECs were starved in 0.5% FBS EBM-2 for 6–8 hr. The cells were treated with TNF-α (0, 0.01, 0.05, 0.1, or 1 ng/mL) for varying periods and/or ACSO (5–30 μg/mL) for 16 hr. The cells treated with dimethylsulfoxide (DMSO)-contained medium were used as solvent controls.

Real Time PCR

Total RNA was extracted from HUVECs using the RNAqueous-4PCR kit. The total RNA (2.5 μg) was reversely transcripted into cDNA using the iScrip cDNA Synthesis Kit. The levels of mRNAs transcripts of the target genes were subsequently assessed by real-time PCR (RT-PCR) (Choi et al., 2004) using the gene-specific primers and iCycler iQ Real-Time PCR Detection System in 96-well reaction plates. The sequences of the primers were forward, 5′-CGACAGTCAGCCGCATCTTC-3′; reverse, 3′-CGCCCAATACGACCAAATCCG-5′ for GAP DH; forward, 5′-TGAACAGAGTGGAAGACATATGCC-3′; reverse, 5′-TCAGATGCGTGGCCTAGTGTT-3′ for ICAM-1, respectively. A total of 50 μL reaction in triplicate was first denatured at 95°C for 3 min and then subjected to 40 cycles of 95°C for 20 sec and 60°C for 1 min. Internal control gene was simultaneously assessed to build the standard curve. The relative levels of mRNA transcripts for the ICAM-1 gene were normalized to that of the GAPDH gene, and the values of cycle threshold (ΔCt) were calculated.

Additionally, the related levels of NOX4 mRNA transcripts were analyzed by RT-PCR using the specific primers, (forward, 5′-ATTTGGATAGGCTCCAGGCAAAC-3′; reverse, 5′-CACATGGGTATAAGCTTTGTGAGCA-3′ for NOX4) and the condition described earlier following treatment of HUVEC cells with TNF-α (0.1 ng/mL) and/or ACSO (10 μg/mL) for 16 hr.

Monocyte Adhesion to HUVECs

The impact of ACSO on TNF-α-induced monocyte adhesion to HUVECs was evaluated as described previously (Christian et al., 1995). Briefly, HUVECs at a density of 2.0×10^5 cells/well were cultured in 10% FBS EBM-2 on a 24-well plate. When reaching 90%–95% of confluence, the cells were starved in 0.5% FBS EBM-2 medium for 8 hr, and then exposed to ACSO (10 μg/mL) for 1 hr, followed by treatment with TNF-α (0.1 ng/mL) for 16 hr. THP-1 cells freshly harvested were labeled with the Calcein-AM (4 μM) in 10% FBS RPMI 1640 medium at 37°C for 30 min. After extensively washing with PBS, the Calcein-AM-labeled THP-1 cells (5.0×10^5 cells/well) were gently added in triplicate into the HUVEC wells that had been treated with ACSO and/or TNF-α, and then incubated at 37°C for 1 hr with gentle shaking. Subsequently, the nonadhered THP-1 cells were gently washed out with 1% FBS PBS and random fields were imaged under a fluorescence microscope using a CCD camera. The numbers of adhered monocytes were counted using the image analysis software (ImagePro) and expressed as the number of adhered cells per field.

Monocyte Adhesion to Porcine Coronary Arteries

The effect of ACSO on TNF-α-induced monocyte adhesion to porcine coronary arterial tissues was examined

as described previously (Chandrasekar et al., 2001). Briefly, porcine hearts were freshly dissected out from farm pigs (6–8-months old) at a local slaughterhouse. The hearts were immediately washed and perfused with cold sterile PBS. Individual right coronary arteries of the hearts were dissected, and the peri-vascular connective tissues were removed. Subsequently, the arteries were divided into 5-mm rings, which were divided randomly into different groups. The rings were treated in triplicate with DMSO (control group), 0.1 ng/mL TNF-α alone, 10 μg/mL ACSO alone or combination of 0.1 ng/mL TNF-α and 10 μg/mL ACSO, respectively, and incubated in 24-well plates (one ring/well) at 37°C and 5% CO_2 for 16 hr. The rings were linearized by one cutting and incubated with Calcein-AM (4 μM)-labeled THP-1 (800 cells/well) for 30 min. The rings were then washed twice with PBS gently and the bound THP-1 cells were visualized under an Olympus BX41 fluorescent microscope (Melville, NY). Adherent monocytes on three fields were selected randomly from each ring and three rings from each group were counted using the ImagePro image analysis software. Data are expressed as the mean number ± SEM of adherent cells per field.

Cellular Superoxide Anion Production

The intracytoplasmic production of superoxide anion was stimulated by TNF-α and measured using the DHE-based FACS analysis, as described previously (Wang and Jordan, 1997). Briefly, HUVEC cells (2.0×10^5/well) were starved for 8 hr as described earlier and treated with TNF-α (0.1 ng/mL), in the presence or absence of ACSO (10 μg/mL), in six-well plates for 16 hr. HUVEC cells treated with 10 μg/mL ACSO or DMSO were used as controls. After washing with PBS, the cells were incubated with 3 μM DHE at 37°C for additional 30 min. Following washing with cold 3% FBS and 0.1% NaN_3 PBS for three times, the cell-bound fluorescence signals were determined by FACS analysis using the FACSCalibur (BD Biosciences). Data were analyzed with the CellQuest software and are presented as net Mean Fluorescence Intensity (MFI) per 10,000 cells or as net percentage of superoxide anion producing cells.

Mitochondrial Membrane Potential Assay

The mitochondrial membrane potential ($\Delta\psi m$) of TNF-α–activated HUVEC cells was measured by the JC-1-based FACS analysis using the MitoScreen (JC-1) kit, according to the manufactures' instructions. Briefly, HUVEC cells (2×10^6 cell/well) were starved for 8 hr and treated with TNF-α (0.1 ng/mL) and/or ACSO (10 μg/mL) for 16 hr. HUVEC cells treated with DMSO were used as control. Subsequently, the cells were incubated with 10 μM JC-1 at 37°C for 15 min. After washing, the intensity of cell staining signals and the frequency of cells with positive mitochondrial staining were determined by FACS analysis using the FACSCalibur. In healthy cells with high mitochondrial $\Delta\psi m$, JC-1 spontaneously forms complexes known as J-aggregates with intense red fluorescence. On the other hand, in apoptotic or unhealthy cells with low $\Delta\psi m$, JC-1 remains in the monomeric form, which shows only green fluorescence. Photomultiplier settings were adjusted to detect JC-1 monomer fluorescence signals on the FL1 detector (green fluorescence, centered at 530 nm) and JC-1 aggregate fluorescence signals on the FL2 detector (red fluorescence, centered at 585 nm). The analyzer threshold was adjusted on the FSC channel to exclude most of the subcellular debris. Cells without dye were used as blank controls. And untreated HUVECs were used as positive controls. Data analyses were performed with Paint-a-Gate Pro Software. As seen in Fig. 5, stained cells can be divided into two populations. The upper left population contains the aggregated form (health cells) and the lower right population contains the monomers (unhealthy cells). We set the gate info based on positive control, and the same gating was used throughout the whole experiment to ensure the consistency. Data analyses were performed with Paint-a-Gate Pro Software (Becton Dickinson). In each experiment, at least 10,000 events were analyzed.

Bio-Plex Luminex Immunoassay

Luminex has been recently used for the evaluation of MAPKs and NF-κB phosphorylation (Cuschieri and Maier, 2005). The impact of ACSO treatment on TNF-α-stimulated phosphorylation of MAPK signaling events and IκB in HUVEC cells were analyzed by Bio-Plex immunoassay using the Bio-Plex Cell Lysis Kit, according to manufacturers' instructions with minor modification (Eyad et al., 2004). Briefly, serum-starved HUVECs were pretreated in triplicate with ACSO (10 μg/mL) for 1 hr and stimulated with 0.1 ng/mL TNF-α for varying periods (0, 2, 5, 10, 15, 30, 45, 60, or 120 min), respectively. The cells were lyzed and the cell lysates were stained with microbeads coupled with the antibody against phosphorylated or total extracellular signal-regulated kinase (ERK1/2), p38, c-Jun N-terminal protein kinase (JNK), IκB or isotype control Ig overnight at room temperature, respectively. After extensive washing, those microbeads were incubated with 25 μL of biotinylated detection antibodies (1×) for 30 min, followed by reacting with streptavidin-PE (1× solution) in the dark for 10 min. After washing, the microbeads were suspended in 125 μL of suspension buffer and the levels of phosphorylated and total ERK1/2, p38, JNK or IκB proteins were analyzed by a Luminex 100 analyzer. The data were analyzed using the Bio-Plex Manager software (BioRad) and are expressed as the mean ± SEM of signal intensity of phosphorylated relative to total protein from three separated experiments.

Statistical Analysis

The data are presented as mean ± SEM. Statistical differences were determined using Student's *t*-test, and a *P*-value <0.05 was considered statistically significant.

RESULTS

ACSO Inhibits TNF-α-Induced Expression of ICAM-1 in HUVECs

The expression of ICAM-1, an important adhering molecule, on endothelial cells can be induced by proinflammatory cytokines, such as TNF-α, which is crucial for the facilitation of inflammatory cells to the sites of atherosclerosis, driving the process of atherosclerotic pathogenesis. To determine the effect of ACSO on the

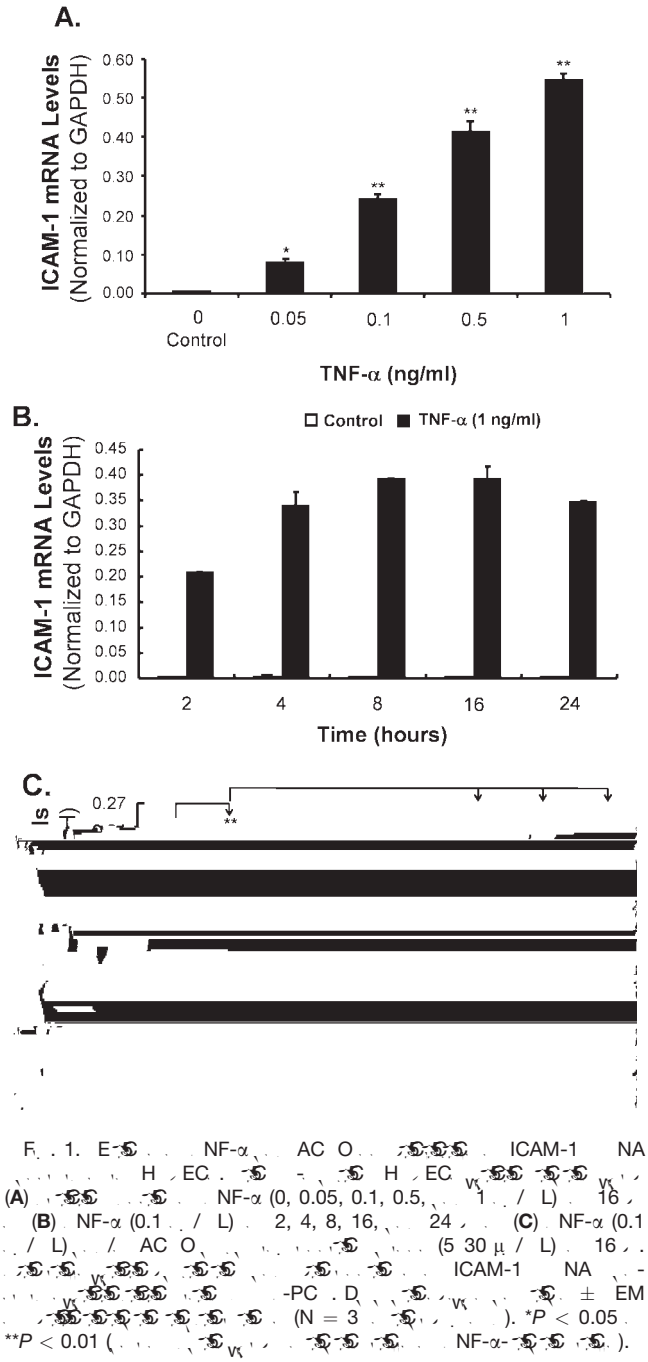

F . 1. E NF-α AC O ICAM-1 NA H EC - H EC v v
(**A**) NF-α (0, 0.05, 0.1, 0.5, 1 / L) 16 (**B**) NF-α (0.1 / L) 2, 4, 8, 16, 24 (**C**) NF-α (0.1 / L) / AC O (5 30 μ / L) 16 ICAM-1 NA - v -PC . D ± EM (N = 3). *P < 0.05 **P < 0.01 (v NF-α-).

expression of TNF-α-induced ICAM-1, we first optimized the conditions for TNF-α to induce ICAM-1 mRNA transcription in HUVECs. As shown in Fig. 1A, TNF-α induced ICAM-1 mRNA transcription in HUVECs in a dose- and time-dependent manner. The relative levels of ICAM-1 mRNA transcripts were elevated as the doses of TNF-α increased and the highest level of ICAM-1 mRNA transcripts was achieved with TNF-α at 1 ng/mL (Fig. 1A). Furthermore, treatment with TNF-α for 2 hr induced significantly higher levels of ICAM-1 mRNA transcripts ($P < 0.01$), as compared with that of untreated controls and extending of TNF-α treatment for a longer period further elevated the levels of ICAM-1 mRNA transcripts in HUVECs (Fig. 1B).

Interestingly, although treatment with ACSO up to 30 μg/mL did not induce significantly higher levels of ICAM-1 mRNA transcripts, ACSO treatment significantly reduced TNF-α-induced ICAM-1 mRNA transcription and its inhibitory effects were dose-dependent (Fig. 1C). In comparison with TNF-α treatment alone, treatment with ACSO at concentrations of 5, 10, or 30 μg/mL decreased the TNF-α-induced ICAM-1 mRNA transcription by 38%, 51%, or 63%, respectively. Therefore, ACSO inhibits the expression of ICAM-1 induced by TNF-α in HUVEC cells *in vitro*.

ACSO Inhibits Monocyte Adhesion to TNF-α-Treated HUVECs and Porcine Coronary Artery Rings

During the pathogenic process of atherosclerosis, monocytes usually adhere to endothelial cells and TNF-α activates endothelial cells, enhancing the adhesion of monocytes. To determine whether ACSO could modulate TNF-α-promoted monocyte adhesion, HUVECs were pretreated with or without ACSO (10 μg/mL) and exposed to TNF-α (0.1 ng/mL), followed by interacting with the Calcein-AM-labeled THP-1 monocytes. The effect of ACSO on THP-1 adhesion to HUVECs was examined (Fig. 2). As expected, there were a few THP-1 cells adhering to HUVEC cells in the absence of ACSO or TNF-α treatment (Fig. 2Aa) and treatment with ACSO alone (Fig. 2Ac) did not change the ability of HUVECs to facilitate THP-1 adhesion as similar numbers of THP-1 cells adhering to HUVEC cells were observed regardless of whether the HUVECs had been treated with or without ACSO. TNF-α treatment (Fig. 2Ab) significantly increased the numbers of THP-1 cells adhering to HUVEC cells ($P < 0.001$). In contrast, pretreatment with ACSO (Fig. 2Ad) significantly mitigated the stimulating activity of TNF-α in promoting THP-1 adhering to HUVEC cells, as the numbers of THP-1 cells adhering to HUVEC cells that had been sequentially treated with ACSO and TNF-α were significantly reduced by 47% as compared with cells treated with TNF-α alone (Fig. 2B). A similar pattern of inhibitory effect of ACSO on TNF-α promoted THP-1 adhering to freshly prepared porcine coronary arterial rings was obtained (Fig. 2C,D). Pretreatment of the rings with ACSO significantly reduced the numbers of THP-1 adhering onto the TNF-α-treated rings by 38%. Therefore, ACSO treatment inhibits monocyte adhesion on TNF-α-activated endothelial cells and artery tissues.

ACSO Reduces TNF-α-Induced Overproduction of Superoxide Anion in HUVECs

Oxidative stress can induce high levels of reactive oxygen species (ROS) production, which contribute to endothelial damage and high permeability (Chen and Keaney, 2004). To investigate whether ACSO treatment could modulate TNF-α-induced overproduction of superoxide anion in HUVECs, cells were treated with TNF-α and/or ACSO and then stained with DHE, a fluorescence dye for superoxide anion, followed by FACS analysis (Fig. 3). The frequency of DHE-stained cells that had been treated with ACSO (51.37%) was similar to that of controls

(53.31%), indicating that treatment with ACSO did not significantly alter the production of superoxide anion in HUVECs. However, ACSO treatment clearly downregulated TNF-α-promoted production of superoxide anion in HUVEC cells *in vitro*. Although 99.52% of HUVECs that had been treated with TNF-α showed DHE-positive, only 69.90% of the cells that had been treated with both TNF-α and ACSO displayed positive for DHE. Importantly, following treatment with ACSO, the average intensity of DHE signals in the cells was reduced from 4×10^2 (TNF-α treated alone) to 10 (treated with both TNF-α and ACSO), near to the point of control cells. Apparently, ACSO not only inhibited the ability of TNF-α to induce high frequency of HUVEC activation, but also downregulated the production of superoxide anion in TNF-α-activated

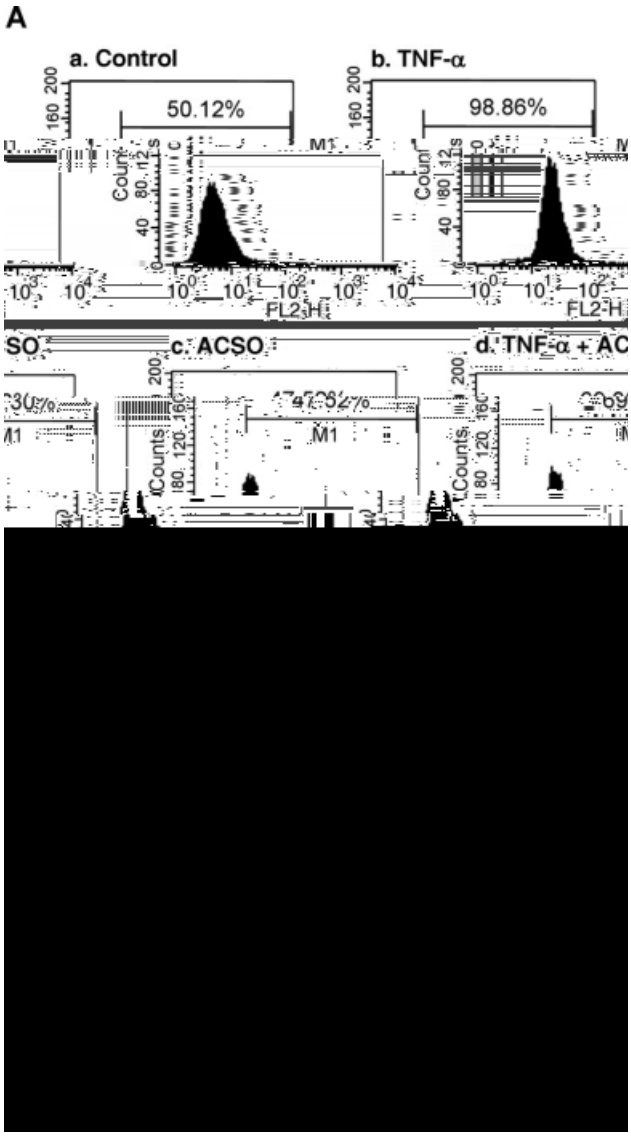

F. . 3. E NF-α AC O H EC . **A**: FAC H EC vs NF-α (0.1 / L) / AC O (10 μ / L) 16 (DHE) 30 - FAC ( ) H EC ; ( ) H EC vs NF-α (0.1 / L) ( ) H EC AC O (10 μ / L) ( ) H EC vs NF-α (0.1 / L) AC O (10 μ / L). B. Q DHE . D vs DHE *$P < 0.05$, NF-α-

expression of NOX4 was determined by quantitative RT-PCT. The relative levels of NOX4 mRNA transcripts in the cells that had been treated with TNF-α (0.1 ng/mL) alone significantly increased by 7.7 folds, as compared with that of controls (Fig. 4). ACSO treatment significantly decreased the levels of NOX4 mRNA transcripts in TNF-α-treated HUVECs, as compared with THF-α alone-treated cells (Fig. 4). Accordingly, ACSO treatment suppressed TNF-α–induced upregulation of NOX4 mRNA transcription in HUVEC cells *in vitro*.

ACSO Inhibits TNF-α-Induced Depolarization of Mitochondrial Membrane Potential in HUVECs

Oxidative stress is usually associated with the depolarization of mitochondrial membrane potential. To determine whether ACSO treatment could inhibit TNF-α-induced depolarization of mitochondrial membrane potential, HUVECs were treated with TNF-α (0.1 ng/mL) and/or ACSO (10 μg/mL) for 16 hr, and the levels of mitochondrial membrane potential were determined by the JC-1-based FACS analysis. As shown in Fig. 5, the cells that had been treated with TNF-α alone displayed higher frequency of cells (R3) with lower mitochondrial membrane potential, an indicative of depolarization, accompanied by lower frequency of cells (R2) with higher mitochondrial membrane potential, as compared with that of control cells. In contrast, treatment with both TNF-α and ACSO significantly reduced the size of depolarized population, accompanied by increasing the frequency of cells with higher mitochondrial membrane potential. Thus, while TNF-α disrupted the mitochondrial membrane potential of HUVECs, treatment with ACSO preserved the mitochondrial membrane potential and prevented TNF-α-induced depolarization in HUVECs *in vitro*.

ACSO Inhibits TNF-α-Induced Activation of JNK and ERK1/2, but Not p38, in HUVECs

TNF-α can bind to its receptors, through the MAPK signaling pathway, and regulate oxidative stress and cell survival. To better understand the mechanism(s) underlying the action of ACSO treatment in HUVECs, the impact of ACSO on TNF-α-induced phosphorylation of MAPKs signaling events was determined by the Bio-Plex immunoassay. HUVEC cells were pretreated with or without ACSO for 1 hr and exposed to TNF-α for indicated time periods (Fig. 6). The levels of phosphorylated and total ERK1/2, JNK, or p38 proteins were analyzed by luminex analysis. Very low levels of phosphorylated protein for each event were detected in the control or the cells that had been treated with ACSO alone (data not shown), suggesting that starved cells cultured in the experimental condition had little MAPK activation and ACSO treatment did not activate the MAPK signaling. However, TNF-α treatment induced phosporylation of ERK1/2, JNK and p38 in HUVECs (Fig. 6A–C) and the highest levels of phosphorlated ERK1/2, JNK and p38 activation displayed 30, 45, or 60 min after TNF-α treatment, respectively. Interestingly, ACSO pretreatment significantly reduced the levels of phosphorylated ERK1/2 and JNK (Fig. 6A,B), particularly at the high peaks. But the treatment did not significantly change the levels of phosphorylated p38 (Fig. 6C). The results suggest that ACSO selectively inhibits TNF-α-induced activation of JNK and ERK1/2, but did not affect p38 phosporylation, in HUVECs.

ACSO Inhibits TNF-α-Induced Activation of NF-κB in HUVECs

NF-κB is one of the major transcription factors, mediating the TNF-α-induced expression of inflammatory molecules (Zhou et al., 2005). NF-κB bound with its inhibitor, IκB, is a ubiquitous inactive molecule in

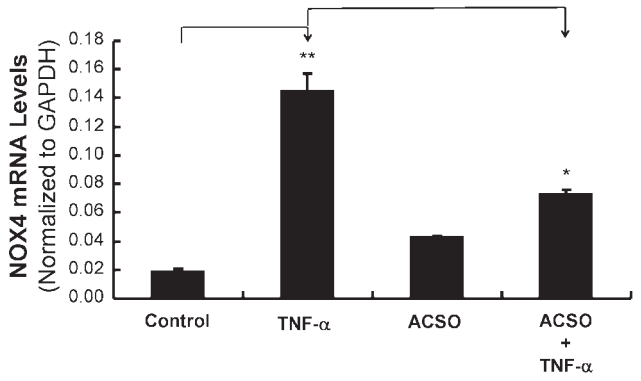

F . 4. E NF-α AC O NO 4 NA H EC H EC NF-α (0.1 / L) / AC O (10 μ / L) 16 NA DNA. NO 4 NA -PC D ± EM NO 4 NA *P < 0.05 **P < 0.01 NF-α-

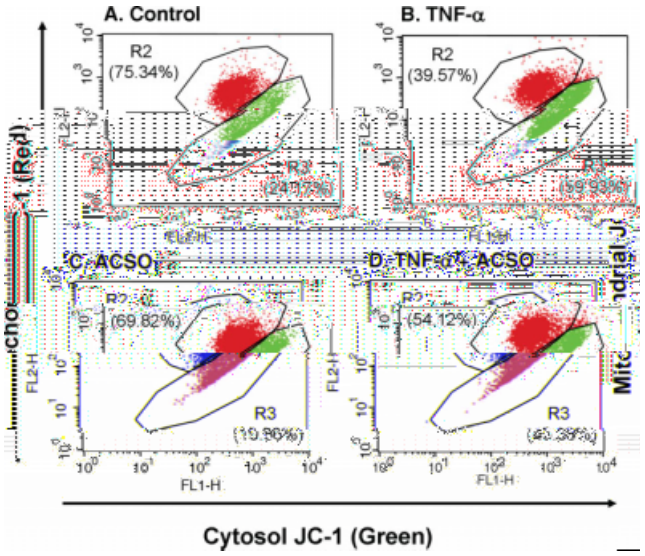

F . 5. E NF-α AC O H EC H EC NF-α (0.1 / L) / AC O (10 μ / L) 16 JC-1 15 ( ) ; ( ) NF-α ( ) AC O ( ) NF-α AC O. (2), ( ) (3). C F C C.

cytoplasma. TNF-α can induce the phosphorylation, ubiquitination and subsequent degradation of IκB proteins and then release the bound NF-κB, which is in turn translocated to the nucleus and induces gene expression (Kumar et al., 1998). Therefore, the level of IκB phosphorylation is an indicative of the activation of NF-κB. To determine whether ACSO could alter the levels of NF-κB activation induced by TNF-α in HUVECs, cells were pretreated with ACSO (10 μg/mL) and then exposed to TNF-α (0.1 ng/mL) for varying durations (0, 2, 5, 10, 15, 30, 45, 60, 120 min). The levels of phosphorylated relative to total IκB proteins were analyzed using Bio-Plex immunoassay. First, very low levels of phosphorylated IκB were detected in control cells and the cells treated with ACSO alone, indicating that ACSO alone did not induce the activation of NF-κB (data not shown). Second, treatment with TNF-α alone promoted high levels of IκB phosphorylation and the highest level of phosphorylated IκB appeared at 60 min post treatment (Fig. 7). Finally, although pretreatment with ACSO did not change the dynamics of TNF-α-induced IκB phosphorylation, ACSO treatment significantly reduced the levels of phosphorylated IκB, particularly at 30–60 min post TNF-α treatment. Hence, ACSO treatment mitigated TNF-α-induced activation of NF-κB in HUVEC cells *in vitro*.

DISCUSSION

Coronary artery disease, such as atherosclerosis, is the most prevalent disease, and a leading cause of morbidity and mortality in many countries (Luscher and Noll, 1994). During the pathogenic process of atherosclerosis, monocytes and other immune cells adhere to endothelial cells of the blood wall. The adhesion, together with inflammatory cytokines such as TNF-α, promotes the migration and proliferation of vascular smooth-muscle cells and the formation of extracellular matrix, which contributes to disease development and progression (Sneddon et al., 2006) The adhesion of monocytes to endothelial cells is likely mediated by intercellular adhesion molecules, such as ICAM-1 and VCAM (Lee et al., 2006). The expression of ICAM-1 can be induced by TNF-α on endothelial cells. And increased ICAM-1 can facilitate the adhesion of monocytes to endothelial cells, and promote the formation of atherosclerostic lesion (Meng et al., 2004; Chung, 2006). We found that TNF-α treatment induced ICAM-1 mRNA transcription in a dose- and time-dependent manner and increased the numbers of THP-1 monocytes adhered onto HUVECs and the porcine coronary arterial rings, consistent with previous reports (Sneddon et al., 2006). Interestingly, treatment with ACSO significantly inhibited the TNF-α-induced ICAM-1 mRNA transcription and monocyte adhesion onto HUVECs and the porcine coronary artery tissues *in vitro*. To our knowledge, this was the first study to show that ACSO treatment effectively inhibited the TNF-α-induced ICAM-1 mRNA transcription and monocyte adhesion.

Free radical species are important regulators for the development of atherosclerosis. Although nitric oxide is crucial for vasodilation of blood vessels, reactive oxygen species (ROS) such as superoxide anion, hydrogen peroxide, and hydroxyl radical, play an important role in the pathogenic process of atherosclerosis (Black, 2004; Van et al., 2005; Cave et al., 2006). The formation of ROS was regulated by intracellular enzymes, such as NADPH oxidase, nitric oxide synthase, lipoxygenase, and cyclooxygenase (Ushio-Fukai, 2006; Miller et al., 2006). ACSO has been shown to have strong antioxidant activity by

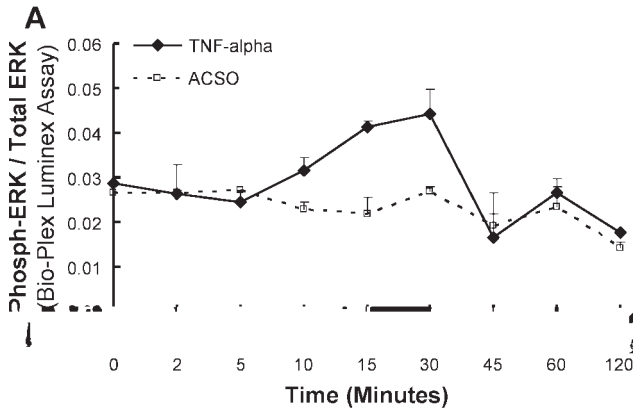

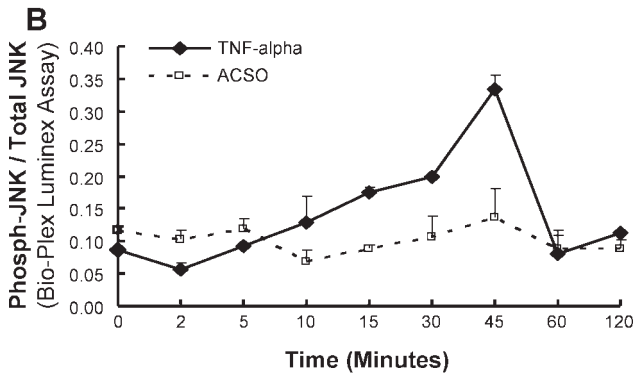

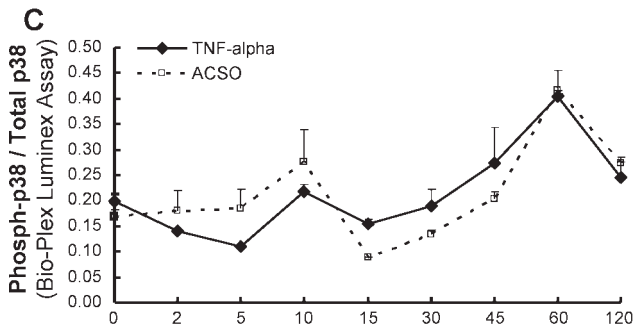

F. . 6. NF-α JNK, E K1/2 38 H EC . H EC AC O (10 μ / L) 1 NF-α (0.1 . / L) (0, 2, 5, 10, 15, 30, 45, 60, 120). MAPK B -P A, B, C E K1/2, JNK, 38, D ± EM DM O AC O ( ).

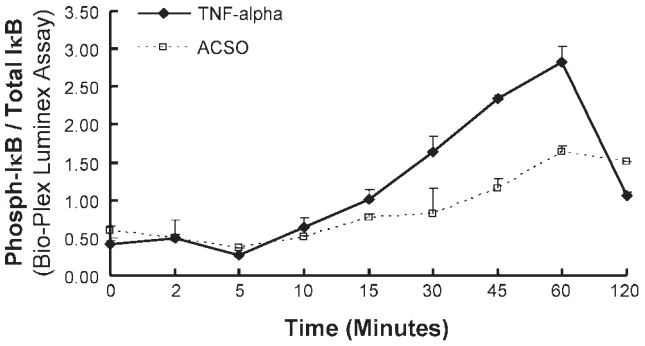

F. . 7. I AC O NF-α IκB H EC IκB B -P . H EC AC O (10 μ / L) 1 NF-α (0.1 / L) (0, 2, 5, 10, 15, 30, 45, 60, 120). IκB B -P . D ± EM IκB IκB DM O AC O ( ).

scavenging hydroxyyl redicals (Salman et al., 1999). We tested whether ACSO could modulate the TNF-α-mediated superoxide anion production in HUVECs and found that treatment with ACSO significantly reduced the TNF-α-mediated superoxide anion production. Furthermore, we found that ACSO treatment dramatically suppressed the TNF-α-mediated upregulation of NOX4 mRNA transcription in HUVEC cells. Indeed, NADPH oxidase and subsequent ROS generation have been described to modulate intracellular signaling, leading to aberrant proliferation or apoptosis, cellular hypertrophy, expression of inflammatory molecules, remodeling of extracellular matrix, or impairment of nitric oxide release (Li and Shah, 2003) Therefore, the reduced levels of NOX4 expression and superoxide anion production in endothelial cells by ACSO may contribute to the protective effect of ACSO on inhibiting the development and progression of atherosclerosis.

Mitochondria is one the most important intracellular component to regulate inflammatory response and survival in endothelial cells and the change in the mitochondrial membrane potential is a sensitive indicator of oxidative stress and inflammation (Nicholls, 2004; Szilagyi et al., 2006). We found that ACSO inhibited the TNF-α-induced depolarization of mitochondrial membrane potential, determined by the JC-1-based FACS analysis (Legrand et al., 2001). As a mitochondrial function marker, decreased $\Delta\psi m$ has been linked to the increase of superoxide anion production and oxidative stress (Plotkowski et al., 2002). Co-treatment of ACSO inhibited superoxide overproduction and reversed ICAM-1 expression induced by TNF-α. Taken together, we believe that ACSO-induced decrease of oxidative stress (shown by restoration of $\Delta\psi m$) maybe the underlying mechanism for ICAM-1 mRNA changes.

The MAPK family is involved in inflammatory factor-mediated signaling (Cuschieri and Maier, 2005). To understand the mechanism(s) underlying the action of ACSO in TNF-α-mediated HUVEC activation, we examined the impact of ACSO treatment on the phosphorylation of ERKl/2, p38 and JNK in HUVECs following treatment with TNF-α *in vitro*. We found that following TNF-α treatment, the relative levels of phosphorylated ERK1/2, JNK and p38 proteins were significantly elevated. However, treatment with ACSO significantly reduced the TNF-α-induced phosphorylation of ERK1/2

and JNK, but not p38. These findings are consistent with previous observation that the ERK1/2 and JNK, but not P38, is involved in the TNF-α-induced endothelial permeability (Kumar et al., 1998; Kuldo et al., 2005). The downregulation of ERK1/2 and JNK phosphorylation should negatively affect downstream JNK activation, which is a crucial regulator for cell activation. Therefore, ACSO is likely to protect endothelial cells from inflammation-triggered ERK1/2 and JNK activation, associated with the inhibition of atherosclerostic progression. However, whether ACSO can directly affect the phosphorylation of ERK1/2 and JNK or indirectly through other factors remains unclear. Further investigations including siRNA knockdown or chemical inhibitor for MAPKs are warranted.

NF-κB is a cytoplasmic component and its activation is the critical process for the downstream activation and gene expression in endothelial cells. TNF-α can induce the phosphorylation of IκB, through its receptor, and result in the activation and translocation of NF-κB to the nucleus, promoting the expression of downstream genes, such as ICAM-1. The activation of NF-κB is also regulated by JNK signaling through inducing β-TrCP and protecting NF-κB from degradation (Kuldo et al., 2005). Furthermore, activation of both NF-κB and JNK together induce a number of gene expressions (Min and Pober, 1997). TNF-α treatment induced higher levels of IκB phosphorylation, which indicative of higher levels of NF-κB activation. We found that treatment with ACSO significantly inhibited the phosphorylation of IκB, suggesting that ACSO treatment inhibited the activation of NF-κB in HUVEC cells *in vitro*. Collectively, we hypothesized that the inhibitory effects of ACSO on monocyte adhesion to HUVEC and porcine coronary arterial rings may be mediated by inhibiting the TNF-α-mediated signaling by suppressing the phosphorylation of ERK1/2 and JNK, as well as the activation of NF-κB by reducing TNF-α-mediated IκB phosphorylation. These in turn mitigate the TNF-α-induced upregulation of ICAM-1 expression and inhibit the TNF-α-induced superoxide anion production by reducing the expression of NOX4 in HUVECs *in vitro*. However, more detailed investigations in the direct link between ACSO-induced ICAM-1 downregulation and decrease of MAPKs and NF-κB are warranted. If proven to be true, ACSO or similar compounds may be beneficial in preventing/inhibiting the development and progression of atherosclerosis.

In summary, our studies presented the first evidence that ACSO treatment effectively reduced TNF-α-induced ICAM-1 mRNA transcription, associated with inhibiting monocyte adhesion to HUVECs and porcine coronary arterial tissues *in vitro*. Furthermore, ACSO protected cells from TNF-α-induced depolarization of mitochondrial membrane potential and overproduction of superoxide anion, which may be associated with the inhibition of NOX4 mRNA transcription in HUVECs. In addition, ACSO treatment mitigated the TNF-α-induced phosporylation of JNK, ERK1/2 and IκB, but not p38, in HUVECs. Therefore, our data may provide new insights into understanding the mechanism(s) underlying the action of ACSO in inhibiting the pathogenic process of atherosclerosis. These findings may aid in design of new therapy for intervention of atherosclerosis and other related cardiovascular diseases.

LITERATURE CITED

Allison MA, Cheung P, Criqui MH, Langer RD, Wright CM. 2006. Mitral and aortic annular calcification are highly associated with systemic calcified atherosclerosis. Circulation 113: 861–866.

Black HS. 2004. ROS: A step closer to elucidating their role in the etiology of light-induced skin disorders. J Invest Dermatol 122:xiii–xiv.

Cave AC, Brewer AC, Narayanapanicker A, Ray R, Grieve DJ, Walker S, Shah AM. 2006. NADPH oxidases in cardiovascular health and disease. Antioxid Redox Signal 8:691–728.

Chandrasekar B, Nattel S, Tanguay JF. 2001. Coronary artery endothelial protection after local delivery of 17β-estradiol during balloon angioplasty in a porcine model: A potential new pharmacologic approach to improve endothelial function. J Am Coll Cardiol 38:1570–1576.

Chen K, Keaney J. 2004. Reactive oxygen species-mediated signal transduction in the endothelium. Endothelium 11:109–21.

Christian W, Wolfgang E, Angelika P, Peter CW. 1995. Aspirin inhibits nuclear factor–B mobilization and monocyte adhesion in stimulated human endothelial cells. Circulation 91:1914–1917.

Choi JS, Choi YJ, Park SH, Kang JS, Kang YH. 2004. Flavones mitigate tumor necrosis factor-alphainduced adhesion molecule upregulation in cultured human endothelial cells: Role of nuclear factorkappa B. J Nutr 134:1013–1019.

Chung LY. 2006. The antioxidant properties of garlic compounds: Allyl cysteine, alliin, allicin, and allyl disulfide. J Med Food 9:205–213.

Cuschieri J, Maier RV. 2005. Mitogen-activated protein kinase (MAPK). Crit Care Med 33:S417–S419.

Eyad E, Paul EW, Howard K, Anthony WR. 2004. Human monocyte isolation methods influence cytokine production from in vitro generated dendritic cells. Immunology 114:204–212.

Hansson GK. 2005. Inflammation, atherosclerosis and coronary artery disease. N Engl J Med 352:1685–1695.

Helen A, Krishnakumar K, Vijayammal PL, Augusti KT. 2003. A comparative study of antioxidants *S*-Allyl cysteine sulfoxide and vitamin E on the damages induced by nicotine in rats. Pharmacology 67:113–117.

Hirsch K, Keren H, Michael D, Judith G, Talia M, Aharon R, Meir W, David M, Joseph L, Yoav S. 2000. Effect of purified allicin, the major ingredient of freshly crushed garlic, on cancer cell proliferation. Nutr Cancer 38:245–254.

Kaperonis EA, Liapis CD, Kakisis JD, Dimitroulis D, Papavassiliou VG. 2006. Inflammation and atherosclerosis. Eur J Vasc Endovasc Surg 31:386–393.

Kuldo JM, Westra J, Kok RJ, Oosterhuis K, Rots MG, Schouten JP, Limburg PC, Molema G. 2005. Differential effects of NF-{kappa}B and p38 MAPK inhibitors and combinations thereof on TNF-{alpha}- and IL- 1{beta}-induced proinflammatory status of endothelial cells in vitro. Am J Physiol Cell Physiol 289:C1229–C1239.

Kumar A, Dhawan S, Aggarwal BB. 1998. Emodin (3-methyl-1,6,8-trihydroxyanthraquinone) inhibits TNF-induced NF-kappaB activation, IkappaB degradation, and expression of cell surface adhesion proteins in human vascular endothelial cells. Oncogene 17:913–918.

Lee DK, Nathan GR, Trachte AL, Mannion JD, Wilson CL. 2006. Activation of the canonical Wnt/beta-catenin pathway enhances monocyte adhesion to endothelial cells. Biochem Biophys Res Commun 347:109–116.

Legrand O, Perrot JY, Simonin G, Baudard M, Marie JP. 2001. JC-1: A very sensitive fluorescent probe to test Pgp activity in adult acute myeloid leukemia. Blood 97:502–508.

Li JM, Shah AM. 2003. ROS generation by nonphagocytic NADPH oxidase: Potential relevance in diabetic nephropathy. J Am Soc Nephrol 14:S221–S226.

Luscher TF, Noll G. 1994. Endothelium dysfunction in the coronary circulation. J Cardiovasc Pharmacol 24 (Suppl 3):S16–S26.

Meng CQ, Somers PK, Hoong LK, Zheng XS, Ye ZH, Worsencroft KJ, Hotema MR, Weingarten MD, Skudlarek JW, Gilmore JM, Hoong LK, Hill RR, Marino EM, Suen KL, Kirsch C, Wasserman MA, Sikorski JA. 2004. Discovery of novel phenolic antioxidants

as inhibitors of vascular cell adhesion molecule-1 expression for use in chronic inflammatory diseases. J Med Chem 47: 6420–6432.

Migita H, Satozawa N, Lin JH, Morser J, Kawai K. 2004. RORα1 and RORα4 suppress TNF-α-induced VCAM-1 and ICAM-1 expression in human endothelial cells. FEBS Lett 557:269–274.

Miller AA, Drummond GR, Sobey CG. 2006. Reactive oxygen species in the cerebral circulation: Are they all bad? Antioxid Redox Signal 8:1113–1120.

Min W, Pober JS. 1997. TNF initiates E-selectin transcription in human endothelial cells through parallel TRAF-NF-kappa B and TRAF-RAC/CDC42-JNK-c-Jun/ATF2 pathways. J Immunol 159: 3508–3518.

Nicholls DG. 2004. Mitochondrial membrane potential and aging. Aging Cell 3:35–40.

Plotkowski MC, Póvoa HC, Zahm JM, Lizard G, Pereira GM, Tournier JM, Puchelle E. 2002. Early mitochondrial dysfunction, superoxide anion production, and DNA degradation are associated with non-apoptotic death of human airway epithelial cells induced by *Pseudomonas aeruginosa* exotoxin A. Am J Respir Cell Mol Biol 26:617–626.

Salman H, Bergman M, Bessler H, Punsky I, Djaldetti M. 1999. Effect of a garlic derivative (alliin) on peripheral blood cell immune responses. Int J Immunopharm 21:589–597.

Sneddon AA, McLeod E, Wahle KW, Arthur JR. 2006. Cytokine-induced monocyte adhesion to endothelial cells involves platelet-activating factor: suppression by conjugated linoleic acid. Biochim Biophys Acta 1761:793–801.

Suwannaprapha P, Chaisri U, Riyong D, Maneerat Y. 2005. Improvement of function and morphology of tumor necrosis factor-alpha treated endothelial cells with 17-beta estradiol: a preliminary study for a feasible simple model for atherosclerosis. Circ J 69:730–738.

Szilagyi G, Simon L, Koska P, Telek G, Nagy Z. 2006. Visualization of mitochondrial membrane potential and reactive oxygen species via double staining. Neurosci Lett 399:206–209.

Ushio-Fukai M. 2006. Localizing NADPH oxidase-derived ROS. Sci STKE 349:re8.

Van Buul JD, Fernandez-Borja M, Anthony EC, Hordijk PL. 2005. Expression and localization of NOX2 and NOX4 in primary human endothelial cells. Antioxid Redox Signal 7:308–317.

Wang M, Jordan SP. 1997. TNF Initiates E-selectin transcription in human endothelial cells through parallel TRAF-NF-KB and TRAF-RAC/CDC42-JNK-c-jun/ATFZ pathways. J Immunol 159: 3508–3518.

Zhou Z, Liu Y, Miao AD, Wang SQ. 2005. Protocatechuic aldehyde suppresses TNF-alpha-induced ICAM-1 and VCAM-1 expression in human umbilical vein endothelial cells. Eur J Pharmacol 513:1–8.